Acta Crystallographica Section B
Structural Science
ISSN 0108-7681

Structural study of the low-temperature phase of TlH_2PO_4 at 180 K

E. Álvarez-Otero,[a] G. Madariaga,[a]* I. Peral,[a] C. L. Folcia[a] and S. Ríos[b]

[a]Materia Kondentsatuaren Fisika Saila, Zientzi-Fakultatea, Euskal-Herriko Unibertsitatea, 644 Postakutxa-48080, Bilbo, Euskadi, Spain, and [b]Department of Earth Sciences, University of Cambridge, Downing Street, Cambridge CB2 3EQ, UK

Correspondence e-mail: wmpmameg@lg.ehu.es

Received 26 October 2001
Accepted 6 June 2002

The low-temperature phase of TlH_2PO_4 has been studied by X-ray diffraction. A structural model is proposed with space group $P\bar{1}$. This model is compared with the structure of the antiferroelectric phase of TlD_2PO_4 at room temperature to analyze the expected isomorphism at low temperature. Given the structural distortion of TlH_2PO_4, such isomorphism present in the common high-temperature phase is not recovered in this phase. Through the analysis of the displacements of the PO_4 groups there is some evidence that the ordering of the H atoms responsible for the appearance of antiferroelectricity seems to be incomplete. An exhaustive study of the detected ferroelastic domains is also performed.

1. Introduction

TlH_2PO_4 (TDP) and its deuterated form TlD_2PO_4 (DTDP) belong to a large family of (anti)ferroelectric materials of the type $A(H,D)_2PO_4$ (with $A = K^+$, Rb^+, Cs^+ *etc.*), of which KH_2PO_4 (KDP) is the most studied. In these compounds, short hydrogen bonds [$R(O—H\cdots O) = 2.4$–2.6 Å] link PO_4 groups in three-dimensional (KDP) or two-dimensional (TDP) networks. One-dimensional (chain) arrangements appear in related compounds like $Pb(H,D)PO_4$. All of them show a remarkable isotope effect as a common characteristic: when the H atoms building their hydrogen-bond system are replaced by D atoms, their Curie temperature (T_c) changes considerably. The reason for this behavior was largely studied during the 1970s, and it was then explained as a consequence of the smaller tunneling power between the double well potential of the asymmetric hydrogen bonds for the deuterium owing to its bigger inertia. The phase transitions at T_c were considered to be a result of the H-atom ordering. Below T_c, H(D) atoms become ordered in one of two possible sites with accompanying movements of the heavy atoms.

Nevertheless, in the 1980s the increasing structural knowledge of these materials showed correlations between the T_c shift and parameters related to the geometry of the hydrogen bonds. In particular, deuteration affects not only the tunneling frequency but also the distances O···O (they are generally larger for the deuterated derivatives) and the proton (deuteron) intersite separation (Lawrence & Robertson, 1980). This is the geometric isotope effect. Consistent with this geometric effect, neutron diffraction under hydrostatic pressure on $Pb(H,D)PO_4$ (McMahon *et al.*, 1990) and $Tl(H,D)_2PO_4$ (Ríos *et al.*, 1999) reveals that the isotope effect disappears when a large enough pressure is applied on the deuterated derivatives. In particular, pressure allows one to study the effect of deuteration at constant O···O distances, *i.e.* at identical potential for H and D. In this case, the value of ΔT_c predicted by considering only proton (deuteron)

tunneling seems to be very large (McMahon *et al.*, 1990). This can be explained (Matsubara & Matsushita, 1984; Blinc & Zeks, 1987) by assuming that the shift in T_c is caused by tunneling through two routes: the different tunneling frequency and the variation of the intersite distances for protons and deuterons.

The theoretical approach based on H(D) tunneling has been questioned by Sugimoto & Ikeda (1991), who have proposed a new model in which no tunneling motion is assumed. Within this approach, the isotope effect (and also the geometric isotope effect) can be explained by a strong coupling between the internal distortion of the PO_4 tetrahedra (which provokes the appearance of an electric dipole moment) and the protons (or deuterons). Therefore, the heavy atoms would participate actively in creating the instability at T_c and the pure order–disorder character of the phase transition should be reconsidered.

On the other hand, it is to be pointed out that the protonated and deuterated forms of the compounds of the $A(H,D)_2PO_4$ family are normally isomorphic before and after the (anti)ferroelectric phase transition. This is not the case for TDP, however, where the isotope effect not only shifts the transition temperature by more than 100 K (T_c^h = 230 K → T_c^d = 353 K)[1] but also leads to a completely different sequence of phase transitions in the temperature range 357–127 K. This sequence can be summarized as follows:

	T_I=357 K		T_c^h=230 K	
Pbcn	⟶	$P2_1/b\ 1\ 1$	⟶	?
a, b, c, Z=4	Ferroelastic	**a, b, c,** Z=4	Antiferroelectric?	
	T_c^d=353 K		T_d=127 K	
Pbcn	⟶	$P1\ 1\ 2_1/b$	⟶	?
a, b, c, Z=4	Antiferroelectric	**2a, b-a, c,** Z=8		

That is, the structural stability of the material changes radically as a consequence of deuteration. From previous structural studies, it is known that TDP and DTDP are isomorphic in their high-temperature phase, with orthorhombic *Pbcn* symmetry and $Z = 4$ (Ríos *et al.*, 1995). However, at a similar temperature [357 K for TDP and 353 K for DTDP (Matsuo & Suga, 1977)] they undergo completely different transitions. TDP undergoes a ferroelastic transition into a $P2_1/b11$ monoclinic structure ($\alpha \simeq 92^\circ$) with the same number of atoms per unit cell (Nelmes & Choudary, 1978; Oddon *et al.*, 1979). This phase transition seems to be triggered by the softening of a PO_4 rigid-body libration mode and involves only a partial ordering of hydrogen bonds. Meanwhile DTDP undergoes an antiferroelectric transition (Yasuda, Fujimoto & Asano, 1980), also into a monoclinic structure, now with the monoclinic axis c and $Z = 8$ (Ríos *et al.*, 1996); the space group can be chosen to be $P112_1/b$ ($\gamma \simeq 107^\circ$) after the change of basis shown in Fig. 1.[2] Unlike the ferroelastic phase transition of TDP, the antiferroelectric transition undergone by DTDP is mainly order–disorder (Ríos, Quilichini & Pérez-Mato, 1998). Nevertheless, the total ordering of D atoms seems to be coupled with the softening of a libration branch of the PO_4 groups.

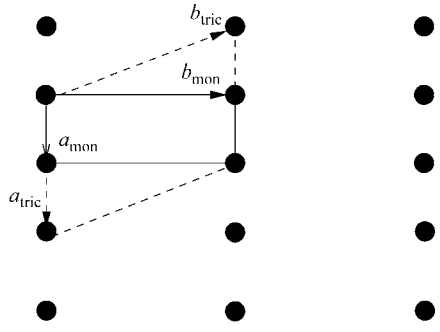

Figure 1
Relation between the monoclinic and triclinic cells of TDP in the *ab* plane.

At a lower temperature [230 K for TDP and 127 K for DTDP (Yasuda, Fujimoto, Asano *et al.*, 1980)], they undergo a second transition to phases whose structure is still a subject of controversy because of the diverse results obtained in different studies. Almost nothing is known about the low-temperature phase of DTDP. For TDP neutron diffraction experiments, Nelmes & Choudary (1981) pointed out a monoclinic structure with space group $P1a1$ and the b axis doubled with respect to that of the room-temperature phase. In a later work, Nelmes (1981) turns this into a $2a \times 2b \times c$ C-centered monoclinic cell. Other X-ray studies (Becker, 1995) suggest a triclinic symmetry with $P\bar{1}$ as the most probable space group. Isomorphism is expected for TDP and DTDP below T_c, and therefore the low-temperature phase of TDP should be antiferroelectric. However, there is no direct evidence of antiferroelectricity in TDP (Yasuda, Fujimoto & Asano, 1980), and therefore its space group has been assigned by analogy with other members of the family. Even isomorphism below T_c^h and T_d (or T_c^d) is uncertain, and an additional phase below 130 K has been proposed for TDP (Pasquier *et al.*, 1997) that would be isostructural with the low-temperature phase of DTDP. Nevertheless, the existence of this additional phase has not been confirmed.

The aim of this work is to clarify this controversy at least partially, proposing a structural model for the low-temperature phase of TDP. The possibility of isomorphism between this low-temperature phase of TDP and the antiferroelectric one of DTDP, as well as the evolution (within the experimental limitations) of the hydrogen bonds across the phase transition, will be analyzed.

[1] Superscripts h and d correspond to the protonated and deuterated compounds, respectively.

[2] Hereafter we will refer to the common orthorhombic phase as the 'high-temperature phase', to the monoclinic structure of each compound as the 'room-temperature phase' and to the still unknown phases as the 'low-temperature phases'. Relevant parameters related to each phase will be denoted with subscripts 'ort', 'mon' and 'tric', respectively.

1.1. The hydrogen-bond system in TDP/DTDP

Owing to the important role that the scheme and evolution of H(D) bonds seem to play in the behavior of this family of materials, we will summarize the previously known structural results concerning TDP (DTDP). Since, for X-rays, H-atom positions are almost invisible in the presence of heavy atoms, we will focus our attention on the changes heavier atoms suffer when H-atom positions become ordered.

There are two types of non-equivalent H(D) atoms in the structure [hereafter denoted H1(D1) and H2(D2)]. H1 atoms link the PO_4 tetrahedra together forming long zigzag-like chains along the *c* axis. H2 atoms link these chains along the *a* axis, forming layers parallel to the *ac* plane (see Fig. 2). Tl atoms are located between the layers, connecting them together. In the orthorhombic prototype phase, H1 and H2 atoms are thought to occupy split (disordered) positions along the O···O line, although they have been refined in special positions (Ríos *et al.*, 1995) with large anisotropic displacement parameters. Also PO_4 groups reveal a strong librational motion. When the temperature is lowered, the ordering of D atoms in DTDP occurs in only one step: both D1 and D2 type atoms become ordered after the antiferroelectric transition at 353 K (Ríos, Paulus *et al.*, 1998). Conversely, the ordering of H atoms in TDP seems to occur in two steps (Seliger *et al.*, 1987); in the monoclinic phase, while H2 type atoms become ordered, H atoms of the H1 type remain dynamically disordered. They are assumed to be ordered after the low-temperature transition. Therefore, it seems that the antiferroelectric character of the transition is given by the H1 atoms and the movement of H2 is only required to follow the displacement of the PO_4 groups. These displacements depend on the ordering of H1 atoms. Tl positions are always strongly pseudosymmetric ($\sim C2/m11$) and practically insensitive to any structural change.

In the monoclinic phase of TDP, the displacement of the PO_4 tetrahedra with respect to the positions they occupy in the high-temperature phase can be described by a rotation of 6.8° around the a_{ort} axis and a small translation along the same axis (Ríos, Paulus *et al.*, 1998). P—O distances corresponding to the O atoms with attached H atoms are slightly larger, and therefore the PO_4 tetrahedra become deformed. In the case of DTDP, PO_4 groups (although they are internally more distorted than in TDP) rotate around both a_{ort} and b_{ort} (Ríos, 1997; Ríos, Paulus *et al.*, 1998).

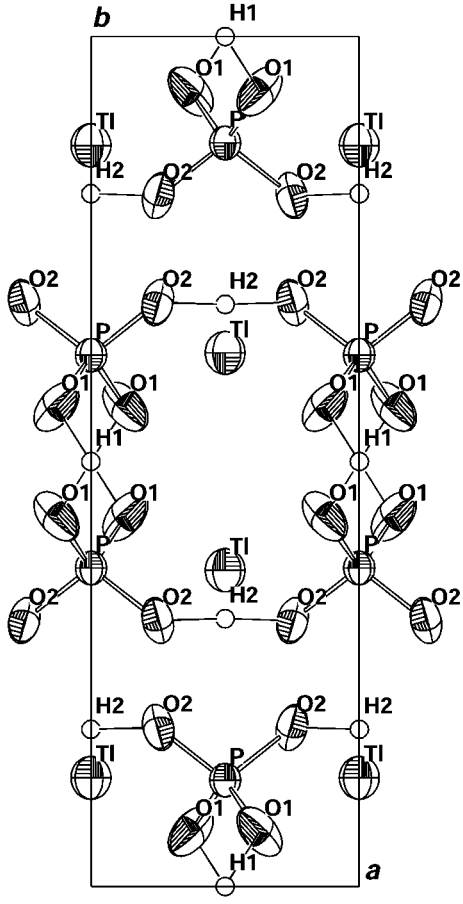

Figure 2
Projection along the c^*_{ort} axis of the structure of TDP in the orthorhombic high-temperature phase. H1 and H2 atoms link the PO_4 tetrahedra along the c_{ort} and a_{ort} axes, respectively.

2. Experimental

The samples employed in all the measurements were synthesized and grown by Ríos *et al.* at L'Université Paris VI and were previously used by this group to study the high-temperature phase using neutron diffraction at the Reactor Orpheé, LLB, Saclay (France). Details of the synthesis and growth are described by Ríos (1997). The samples were rather large ($\sim$1 cm^3) and needle-shaped along the a_{mon} axis. Samples suitable for X-ray measurements ($\sim$0.1 mm) were obtained by carefully cutting on the cleavage planes, but they lacked a well defined morphology.

Data collection was performed with a Stoe IPDS (Stoe, 1998) X-ray diffractometer. A summary of the crystal data and data collection parameters is given in Table 1. Monochromatic Cu $K\alpha_1$ X-ray powder measurements were carried out on a Stoe focusing beam transmission diffractometer equipped with a linear position-sensitive detector. Samples were prepared by pulverization of the synthesized single crystals. Powder diffraction patterns were collected using Debye–Scherrer geometry. The scanned region of reciprocal space was 5–100° in 2θ. Temperature was controlled with an Oxford Cryostream (Cosier & Glazer, 1986) cooling system. Temperature stability was within $\pm$0.2 K. To test the quality of the samples, we performed some measurements at room temperature. The structure could be refined without problems (R = 4.3%), and the results agree with those already published by Nelmes & Choudary (1981). Regarding the lattice parameters of the low-temperature phase, TDP undergoes at 230 K a very similar change to that in DTDP at 353 K in which the a_{mon} axis is doubled. However, a small shear of about 0.6° in the *ab* plane also occurs in TDP, which invalidates the possibility that the crystal class remains unchanged in this phase as suggested by Nelmes & Choudary (1981). This shear,

Table 1
Experimental details.

Crystal data	
Chemical formula	TlH_2PO_4
Chemical formula weight	301.34
Cell setting, space group	Triclinic, $P\bar{1}$
a, b, c (Å)	8.997 (5), 14.866 (6), 6.499 (3)
α, β, γ (°)	92.03 (3), 89.92 (6), 107.01 (4)
V (Å^3)	830.7 (7)
Z	8
D_x (Mg m^{-3})	4.818
Radiation type	Mo $K\alpha$
μ (mm^{-1})	39.141
Temperature (K)	180.0 (2)
Crystal form, color	Irregular, colorless
Sample volume (mm^3)	0.125
Data collection	
Diffractometer	Imaging plate
Data collection method	φ-rotation scans
Distance IPDS (mm)	70
2θ range (°)	3.3–52.1
No. of exposures	180
φ range (°)	0–360
φ increment (°)	2
Irradiation/exposure (min)	3
Profile function	Dynamic
Smallest, largest profile diameter (pixel)	11, 29
Effective mosaic spread	0.01
Data set completeness (%)	100
Data set redundancy	1.95
Absorption correction	Gaussian
T_{min}	0.0066
T_{max}	0.0455
No. of measured, independent and observed reflections	6004, 3017, 1504
Criterion for observed corrections	$I > 3\sigma(I)$
R_{int}	0.0850
θ_{max} (°)	26.02
Range of h, k, l	$-10 \rightarrow h \rightarrow 11$ $-18 \rightarrow k \rightarrow 18$ $-7 \rightarrow l \rightarrow 7$
Refinement	
Refinement on	F^2
$R[I > 3\sigma(I)$ on $F^2 > 3\sigma(F^2)]$, $wR(F)$, S	0.0631, 0.1801, 1.32
$R[F]$, $h = 2n$	0.0671
$R[F]$, $h = 2n + 1$	0.0532
No. of reflections and parameters used in refinement	3017, 127
Weighting scheme	$w = 1/[\sigma^2(I) + 0.0036I^2]$
$(\Delta/\sigma)_{max}$	0.2400
$\Delta\rho_{max}$, $\Delta\rho_{min}$ (e Å^{-3})	5.76, −5.2
Refined twin volume fraction	0.447 (4)

Computer programs used: Stoe *IPDS* (Stoe & Cie, 1998), *JANA*2000 (Petrícek & Dusek, 2000), *FullProf* (Rodriguez-Carvajal, 1999), *ORTEP* (Davenport *et al.*, 2000).

which transforms γ by 90.6°, combined with the inherited value of 92° for α (slightly larger than at room temperature) confirms that the system is triclinic. For a better comparison with the monoclinic structure of DTDP, the cell parameters were redefined ($a_{tric} = 2a_{mon}$, $b_{tric} = b_{mon} - a_{mon}$, $c_{tric} = c_{mon}$) as in Fig. 1.

2.1. Description of the reciprocal space

The reciprocal space at 180 K shows mostly the same characteristics as that at 293 K, excluding the presence of some new very faint reflections that break the $P2_1/b11$ symmetry and the appearance of very weak superstructure reflections (see Fig. 3) indicating that the structural distortion is small in amplitude. For instance, the intensity of the reflection $(\bar{6}80)$ is about six times that of $(\bar{5}80)$. This ratio between the intensities of the reflections with h even and odd can be extrapolated to the rest of the reflections. Therefore, it seems that the structural changes are not very important, and the low-temperature structure will show a strong pseudosymmetry. This causes the existence of (pseudo)systematic absences that characterize the reciprocal space through the whole of the temperature range (293–180 K). The most remarkable is that observed in the ($hk0$) plane (to a lesser extent it is also observed in other parallel layers) along directions parallel to b^*_{tric}, in which one reflection (fulfilling the condition $h + k = 2n + 1$, where n is an integer) out of four is absent (Fig. 3). All of these pseudo-absences can be explained by considering the Tl and P positions[3] (see supplementary material[4]). The strong diffraction power of these atoms dominates the structure factor and enhances the importance of the pseudosymmetry that hinders the assignation of a space

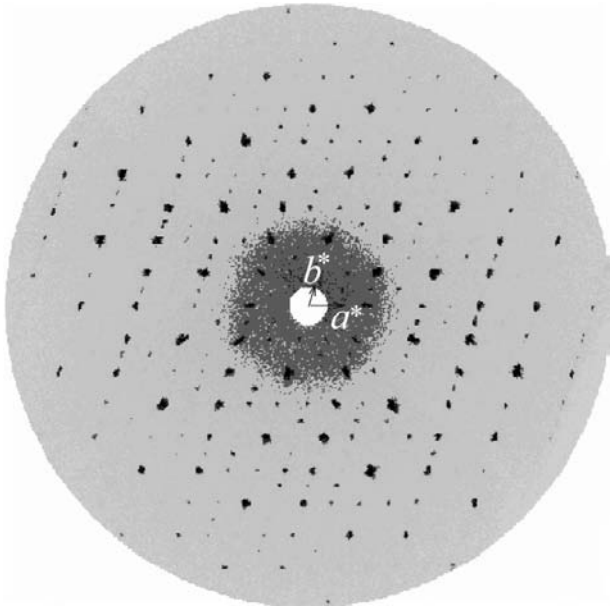

Figure 3
($hk0$) plane of TDP at 180 K. The superstructure reflections with $h = 2n + 1$ are much weaker than those that still preserve a high orthorhombic pseudosymmetry. The strong pseudosymmetry showed by the heavy atoms (see text) provokes the appearance of (pseudo)systematic absences. For example, in several reciprocal rows parallel to b^*_{tric} one reflection out of four is absent.

[3] After an inverse change of basis, $a_{mon} = a_{tric}/2$, $b_{mon} = b_{tric} + a_{tric}/2$, the supplementary material shows clearly that Tl and P atoms remain nearly immobile in positions showing a very strong pseudosymmetry. $C2/m11$ is easily detected. In addition, Tl and P positions are related by symmetry elements ($P2_1/b11$) inherited from the higher-temperature phase together with pseudo-centering translations like (weaker) [0,1/4,1/2] or pseudo glide planes like $\{\sigma_z|1/2,1/4,0\}$.

[4] Supplementary data for this paper are available from the IUCr electronic archives (Reference: NA0131). Services for accessing these data are described at the back of the journal.

group for the whole structure. On the other hand, the (0*kl*) reciprocal plane (Fig. 4*a*) exhibits the existence of twinning. There is a clear reflection splitting for $2\theta \geq 18^\circ$ that increases with the Bragg angle. The two domains are related by a mirror plane perpendicular to the c_{ort} axis. Although TDP crystals are known to grow with inherent twins (Yoshida *et al.*, 1984), the twin law is different from the one observed. Therefore, the detected twin domains arise as a consequence of a spontaneous shear strain. Since the same splitting is observed at room temperature (although it is less notorious because $\alpha = 91.5^\circ$), this twinning can be explained by considering that in the ferroelastic phase transition ($Pbcn \rightarrow P2_1/b11$) two mirror planes, perpendicular to b_{ort} and to c_{ort}, are lost. This symmetry reduction enables the existence of two ferroelastic domains, which should provoke a reflection splitting in the (0*kl*) plane, with reflections separated by $2\Delta\alpha^*$, where $\Delta\alpha^* = \alpha^*_{ort} - \alpha^*_{mon}$. An analysis of the diffraction spots shows that the reflections corresponding to one of these two domain states are clearly more intense than those corresponding to the other. A closer inspection of the (0*kl*) spots shows that their shape varies over the plane: they are sharper for small 2θ values and become wider in the off-center regions. In fact, these wide reflections are formed by two unresolved maxima. In Fig. 4(*b*), an amplified picture of two of these spots is shown in which the four maxima are obvious. This additional splitting cannot be foreseen using the simple approach for calculating the orientation of domain walls given above and will be discussed in depth in the next section. However, the same argument can be extrapolated to the second phase transition ($P2_1/b11 \rightarrow P\bar{1}$ assuming the low-temperature phase is centrosymmetric), which is supposed to be antiferroelectric and involves the loss of a glide plane perpendicular to *a*. It should provoke an additional splitting in the (*hk*0) reciprocal plane. Its presence is more difficult to detect ($\Delta\gamma^* = 0.6^\circ$) and it has only been detected in a few reflections [see Figs. 5(*b*) and 5(*d*)]. Such results contradict the conclusions of a previous optical study (Kim *et al.*, 1998) where the symmetry of this phase is stated as monoclinic.

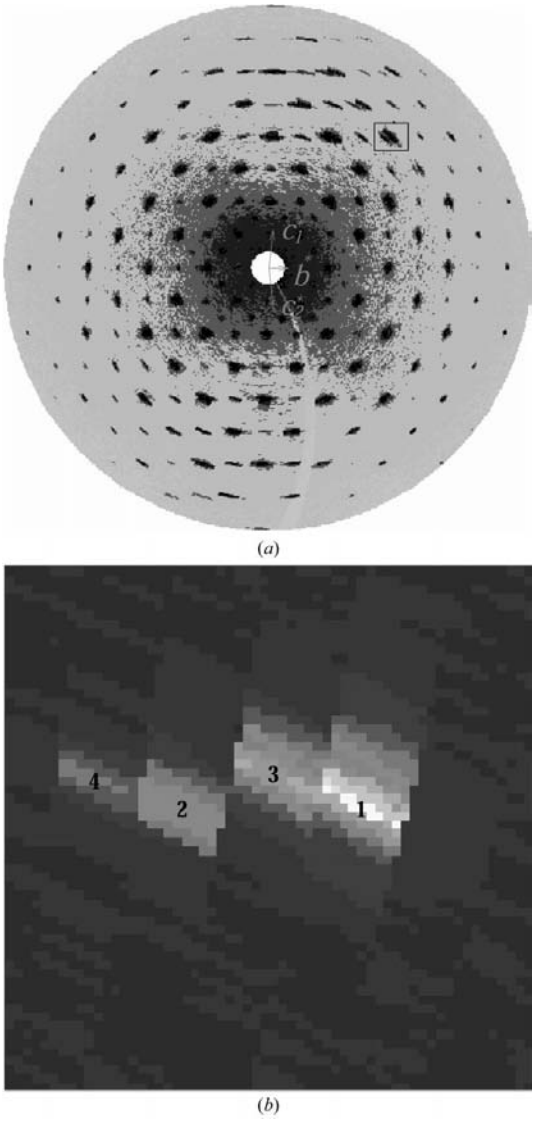

Figure 4
(*a*) (0*kl*) plane of TDP at 180 K. Reflections with $k = 2n + 1$ are absent owing to pseudosymmetry. Reflection splitting reveals two ferroelastic domains. Their b^* and c^* axes are sketched. (*b*) Enlargement of the marked area showing domains slightly disoriented. Spots 1 and 2 belong to two domains related by a plane perpendicular to c_{ort}; 3 and 4 come from two domains related by a plane tilted (with respect to that relating 1 and 2) $\sim 2^\circ$ around a_{ort}.

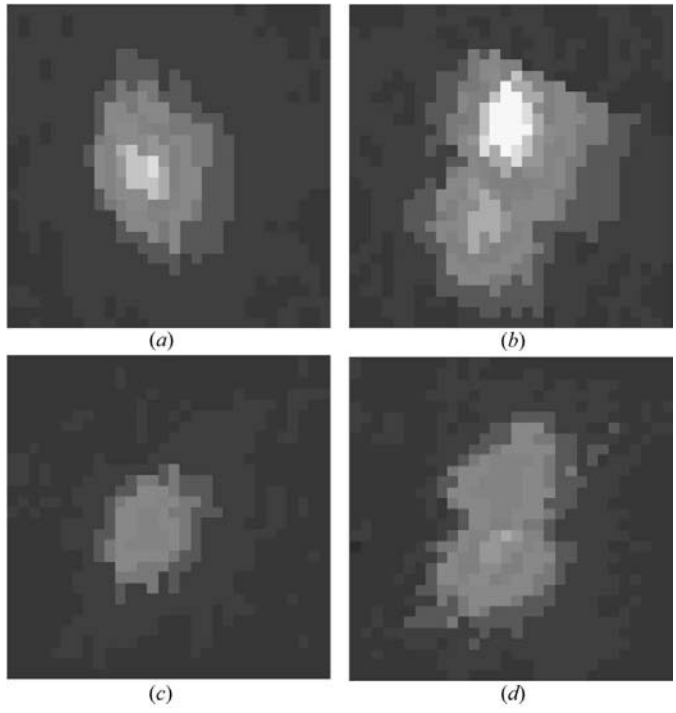

Figure 5
Evidence of the splitting of reflections in the (*hk*0) plane, arising from the presence of new ferroelastic domains derived from the loss of a glide plane perpendicular to a_{mon} in the phase transition $P2_1/b11 \rightarrow P\bar{1}$. (*a*) Reflection $(330)_{mon}$ at 293 K, before the phase transition. (*b*) Same reflection $(600)_{tric}$ at 180 K, where the splitting in two is obvious. (*c*) and (*d*) represent the same for reflections $(370)_{mon}$ and $(6\bar{1}00)_{tric}$, respectively.

Altogether, and despite the strong pseudosymmetries mentioned previously, the symmetry of the reciprocal space is most probably triclinic. However, macroscopic measurements are necessary to decide which is the correct space group. In this respect, second-harmonic generation measurements were performed in order to check the non-existence of inversion in the point group of TDP at the low-temperature phase. The measurements were carried out using a Q-switched Nd3+:YAG laser (wavelength $\lambda = 1064$ nm, pulse width 6 ns, pulse frequency 5 Hz). The experimental setup included an Oxford Cryostream (Cosier & Glazer, 1986) cooling system, which allowed a continuous detection of the second-harmonic light ($\lambda = 532$ nm) *versus* temperature. No signal was detected on cooling the crystal to the low-temperature phase. This strongly suggests the existence of an inversion center, and therefore $P\bar{1}$ was chosen as the space group of the low-temperature phase of TDP.

3. Study of the ferroelastic domains

Shuvalov (1985) set a valuable formalism to calculate the position of domain walls. This approach gives the boundaries derived from symmetry considerations [see, for example, Sapriel (1975)] and may also calculate some slightly rotated new boundaries. The rotation angles, φ, can be derived from the eigenvalues of $x_s(S_1) - x_s(S_2)$, where $x_s(S_1)$ and $x_s(S_2)$ are the spontaneous strain tensors of two adjacent orientational states. Hence φ is temperature dependent.

In our case, part of the domains [those that provoke the splitting of the $(0kl)$ plane] are generated in the high-temperature ferroelastic transition, which belongs to the *mmmF*2/*m* Aizu class) (Aizu, 1970). Setting the twofold axis along the $a_{\rm ort}$ axis, the form of the strain tensors corresponding to the two possible orientational states is the following:

$$x(S_1) = \begin{pmatrix} e_{11} & 0 & 0 \\ 0 & e_{22} & e_{23} \\ 0 & e_{23} & e_{33} \end{pmatrix}, \tag{1}$$

$$x(S_2) = \begin{pmatrix} e_{11} & 0 & 0 \\ 0 & e_{22} & -e_{23} \\ 0 & -e_{23} & e_{33} \end{pmatrix}, \tag{2}$$

where, according to Salje (1990),

$$e_{11} = \frac{a\ \sin\gamma}{a_0\ \sin\gamma_0} - 1, \tag{3}$$

$$e_{22} = \frac{b}{b_0} - 1, \tag{4}$$

$$e_{33} = \frac{c\ \sin\alpha\ \sin\beta_0}{c_0\ \sin\alpha_0\ \sin\beta_0^*} - 1, \tag{5}$$

$$e_{23} = \frac{1}{2}\left[\frac{c\cos\alpha}{c_0 \sin\alpha \sin\beta_0^*} + \frac{\cos\beta_0^*}{\sin\beta_0^* \sin\gamma_0} \times \left(\frac{a\cos\gamma}{a_0} - \frac{b\cos\gamma_0}{b_0}\right) - \frac{b\cos\alpha_0}{b_0 \sin\alpha_0 \sin\beta_0^*}\right]. \tag{6}$$

a, b, c, α, β and γ are the cell parameters of the ferroelastic phase, and a_0, b_0, c_0, α_0, β_0 and γ_0 are the cell parameters corresponding to a hypothetical orthorhombic structure extrapolated from the high-temperature phase. The values are usually extrapolated by defining an average structure whose strain tensor is the arithmetic mean of all possible strain tensors of the low-symmetry phase:

$$x_{\rm av} = \frac{1}{2}[x(S_1) + x(S_2)] = \begin{pmatrix} e_{11} & 0 & 0 \\ 0 & e_{22} & 0 \\ 0 & 0 & e_{33} \end{pmatrix}. \tag{7}$$

In the average structure, the tensor components are identically zero ($e_{11} = e_{22} = e_{33} = 0$). Therefore, according to (1), (2) and (3), $a_0 = a \sin\alpha$, $b_0 = b$ and $c_0 = c \sin\alpha$. Hence the spontaneous strain tensors and their difference are

$$x_s(S_1) = \begin{pmatrix} 0 & 0 & 0 \\ 0 & 0 & e_{23} \\ 0 & e_{23} & 0 \end{pmatrix}, \tag{8}$$

$$x_s(S_2) = \begin{pmatrix} 0 & 0 & 0 \\ 0 & 0 & -e_{23} \\ 0 & -e_{23} & 0 \end{pmatrix}, \tag{9}$$

$$\Delta x = x_s(S_1) - x_s(S_2) = \begin{pmatrix} 0 & 0 & 0 \\ 0 & 0 & 2e_{23} \\ 0 & 2e_{23} & 0 \end{pmatrix}. \tag{10}$$

From (10) and (6), the rotation angles for the ferroelastic domains can be calculated to be $\varphi = 0, \pm 2e_{23}$ ($= \pm 2.23^\circ$), in good agreement with the experimental values [compare Figs. 4(*a*) and 4(*b*) with Fig. 6]. There is no evidence of additional reflection splitting in the $(hk0)$ plane.

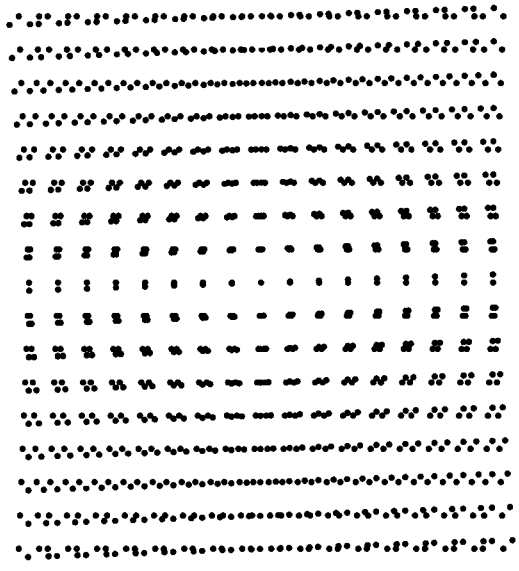

Figure 6
Theoretical $(0kl)$ plane of TDP where the four ferroelastic domains detected in reciprocal space are present.

4. A structural model for the low-temperature phase of TD

4.1. Refinement of the structure

There are two main problems in this case regarding the partial superposition of reflections belonging to different domains. First, the spots related by the tilted domain walls in the (0*kl*) plane can hardly be resolved. This means that all of the integrated intensities contain information about the two domains, so the refinement is difficult to handle. Hopefully the volume fraction of one of the domains can be considered almost negligible (see Fig. 4*b*). Second, the partial superposition of the spots corresponding to domains related by the mirror planes (perpendicular to a_{mon} and c_{ort}) implies that there are regions where the intensities have different contributions from each orientational state. After different trials, we opted to integrate the intensities choosing only the orientation matrix of one of the twin domains with a profile function width dependent on the Bragg angle. Any attempts to use other options or to separate these contributions failed. Furthermore, the mutual screening of the different domains in a highly absorbent material like TDP makes the absorption correction systematically biased.

Additional difficulties arise from the strong pseudosymmetry showed by the heavy atoms (an average structure was still refineable in the higher-temperature space group $P2_1/b11$ up to an agreement factor of 6.85%) and the consequence that they almost do not contribute to the weak superstructure reflections that carry the information about the cell duplication that is practically caused by O-atom displacements. Finally, it should be noted again that the strong scattering power of the Tl atoms hides the contribution to the structure factor of the other atoms, especially the H atoms.

The refinement was performed with *JANA*2000 (Petrícek & Dusek, 2000). Atoms were incorporated into the model in order of decreasing atomic number. First, only the atomic coordinates (derived from our own results of the room-temperature phase) and an isotropic displacement parameter were refined for Tl and P atoms. Anisotropization of the displacement parameters was only possible in the case of Tl. For these two types of atoms, a clear decrease of U_{equiv} is observed with respect to the monoclinic phase. Nevertheless, this decrease does not strictly follow the expected linear law of *U versus T*, probably because of the strong correlation among the atoms that are related by symmetry in the high-temperature phase. As expected, Tl and P atoms remain almost immobile in their initial positions. Once the P atoms were refined, the O atoms were introduced in successive cycles, grouping them in different tetrahedra. During the first cycles of refinement, each PO_4 tetrahedron was considered as a rigid molecule. Once convergence was virtually reached, this restriction could be suppressed. P and O atoms related by the symmetry operations of the monoclinic phase were restrained to have the same temperature factor. If this restriction is not applied, the isotropic displacement parameters range between 0.008 Å^2 and 0.05 Å^2.

The twin laws corresponding to the symmetry operations lost in the successive phase transitions were tested during the refinement. The refined relative volumes were 0.7 (11)% and 44 (1)% for the mirror planes perpendicular to c_{ort} and a_{mon}, respectively. However, the spots corresponding to each orientational state seem to have intensities within the same order of magnitude, *i.e.* their volumes should not be as different as the refined fractions indicate. The reason for this contradiction may be that the splitting in the (0*kl*) plane is large enough for integrating separately the intensities of each domain at least for $\sin\theta/\lambda > 0.36$. Nevertheless, this assumption could not be confirmed refining the volume fractions in selected ranges of $\sin\theta/\lambda$. In the (*hk*0) plane, the spots are so close that each reflection contains complete information about each orientational state, and therefore the volume fraction is much more realistic. Accordingly, the twin law corresponding to the plane perpendicular to c_{ort} was removed.

The inclusion of the twin law is significant [$R(F)$ reduces by 5%] and influences the positions of the O atoms. Any attempt to refine the positions of the O atoms using only superstructure reflections failed. The final $R(F)$ is 6.31% for all reflections (6.71% and 5.32% for those with $h = 2n$ and $h = 2n + 1$, respectively).

The refined atomic parameters are listed in the supplementary material. A projection of the triclinic structure along c^*_{tric} is shown in Fig. 7. In spite of the relatively high R factor, a different refinement run starting from the antiferroelectric structure of DTDP shows that the solution is stable. The relatively high residual Fourier peaks very close to Tl atoms (< 1 Å) seem to be a truncation effect of the Fourier series.

To avoid the effects of the ferroelastic domains, powder diffraction measurements were also performed for this compound at 180 K. The indexation was difficult owing to the low symmetry of the structure. A Rietveld refinement was carried out with *FullProf* (Rodriguez-Carvajal, 1999). The final atomic positions (not including H atoms) agree with those in the supplementary material.

As expected, H atoms could not be detected in difference Fourier maps. Nevertheless, the pairs of O atoms involved in hydrogen bonds are easily found. P—O···O angles are in the interval [113 (2)°, 124 (2)°], which is very similar to those found at room temperature [122.03 (19)°, 124.7 (2)°] (Ríos *et al.*, 1995), in the antiferroelectric phase of DTDP [118.22°, 123.86°] (Ríos, Paulus *et al.*, 1998) or in KDP [112.75 (1)°] (Nelmes *et al.*, 1982). In these compounds, H(D) atoms practically lie on the line joining each pair of O atoms.

Several models of hydrogen bonds were tested. All of them required very strong restrictions in the coordinates of the H atoms and fixed temperature factors. Initially, O—H distances were allowed to vary in the range 1.0–1.5 Å without any restriction in the O—H···O angle. The result showed an unreliable scheme of hydrogen bonds. The lack of resolution of X-ray diffraction refinements regarding the position of the H atoms motivated the use of other techniques to obtain information about the hydrogen bonds. The maximum entropy method shows a distribution of (possible) H atoms that is clearly unreliable and confirms that there is almost no infor-

Table 2
Bond valences (v.u.) of atoms involved in hydrogen bonds.

Atom	Valence	Atom	Valence	Atom	Valence	Atom	Valence
O_{1a}	2.2 (7)	O_{2a}	2.2 (2)	O_{3a}	2.3 (8)	O_{4a}	2.0 (2)
O_{1b}	1.96 (15)	O_{2b}	2.2 (9)	O_{3b}	1.7 (2)	O_{4b}	2.6 (5)
O_{1c}	1.9 (2)	O_{2c}	2.4 (7)	O_{3c}	2.1 (2)	O_{4c}	2.2 (5)
O_{1d}	2.5 (3)	O_{2d}	1.56 (19)	O_{3d}	2.6 (11)	O_{4d}	1.9 (2)
H_{1a}	1.1 (7)	H_{1b}	1.1 (9)	H_{1c}	1.1 (3)	H_{1d}	1.1 (11)
H_{2a}	1.1 (5)	H_{2b}	1.1 (5)	H_{2c}	1.2 (9)	H_{2d}	1.1 (7)

mation about the H atoms in the measured intensities. Also, bond valence calculations (Brese & O'Keefe, 1991) were performed to improve the positions of the H atoms[5] obtained in the refinement. However, an analysis of the standard uncertainties for valences (see Table 2) shows that any improvement in the positions of H atoms is impossible. Finally, H-atom positions were restricted to conform a network of almost linear hydrogen bonds similar to that of the antiferroelectric phase of DTDP (including the donor/acceptor character of the bonded atoms since it cannot be inferred from

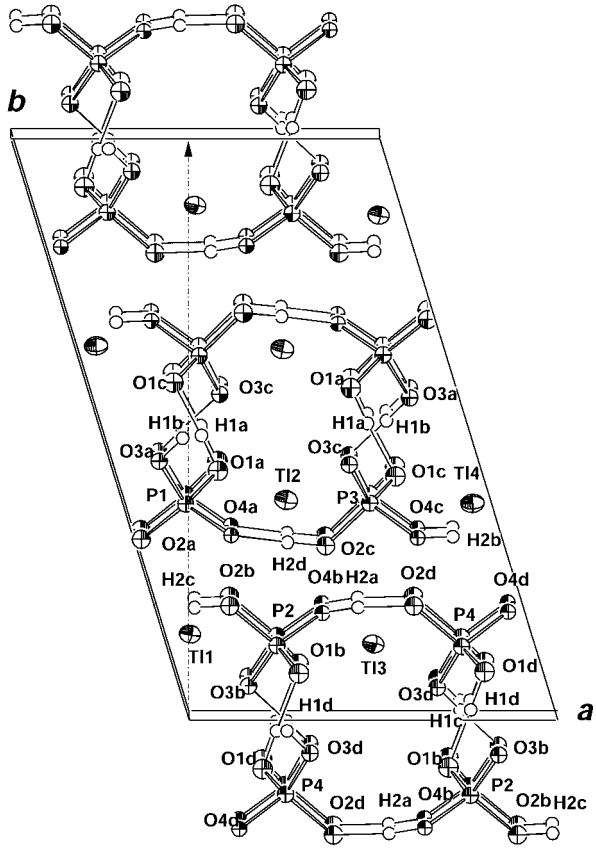

Figure 7
Projection along the c^*_{tric} axis of the low-temperature structure of TDP. The dotted line indicates the direction of b_{mon} and b_{ort}. The hydrogen-bonding scheme is similar to that found in the antiferroelectric phase of DTDP (see Fig. 8 for an alternative hydrogen-bond distribution as derived from force-field calculations).

[5] Bond valences for H atoms were estimated in the usual form, although it is known that such calculations (Brown & Altermatt, 1985) could be inaccurate.

Table 3
Selected interatomic distances (Å) and angles (°) for TDP at 180 K.

Both schemes (see text) of hydrogen bonding are included. Notice that force-field calculations restrict the O—H distance to 0.85 Å and the P—O—H angle to 109°. See the supplementary material for atom labeling.

P_1-O_{1a}	1.62 (3)	$O_{1a}-H_{1a}$	1.0 (3)
P_1-O_{2a}	1.46 (4)	$O^{i}_{1c}-H_{1a}$	1.5 (3)
P_1-O_{3a}	1.56 (4)	$O_{3a}-H_{1b}$	1.0 (3)
P_1-O_{4a}	1.52 (4)	$O^{ii}_{3c}-H_{1b}$	1.5 (3)
P_2-O_{1b}	1.51 (4)	$O^{iii}_{1d}-H_{1c}$	1.00 (12)
P_2-O_{2b}	1.58 (5)	$O_{1b}-H_{1c}$	1.56 (13)
P_2-O_{3b}	1.53 (3)	$O^{iv}_{3d}-H_{1d}$	1.0 (4)
P_2-O_{4b}	1.50 (3)	$O_{3b}-H_{1d}$	1.6 (4)
P_3-O_{1c}	1.55 (3)	$O^{v}_{4b}-H_{2a}$	1.0 (2)
P_3-O_{2c}	1.53 (3)	$O^{v}_{2d}-H_{2a}$	1.5 (2)
P_3-O_{3c}	1.47 (4)	$O^{vi}_{4c}-H_{2b}$	1.0 (2)
P_3-O_{4c}	1.57 (4)	$O_{2a}-H_{2b}$	1.5 (2)
P_4-O_{1d}	1.55 (4)	$O^{v}_{2b}-H_{2c}$	1.0 (3)
P_4-O_{2d}	1.63 (5)	$O^{vii}_{4d}-H_{2c}$	1.5 (3)
P_4-O_{3d}	1.50 (3)	$O^{vi}_{2c}-H_{2d}$	1.0 (3)
P_4-O_{4d}	1.52 (3)	$O^{vi}_{4a}-H_{2d}$	1.6 (3)
$O_{1a}-O^{i}_{1c}$	2.50 (5)	$O_{3a}-O^{ii}_{3c}$	2.52 (5)
$O_{1b}-O^{iii}_{1d}$	2.56 (4)	$O_{3b}-O^{iv}_{3d}$	2.57 (6)
$O_{2a}-O^{vi}_{4c}$	2.49 (5)	$O_{4a}-O_{2c}$	2.58 (6)
$O_{2b}-O^{vi}_{4d}$	2.45 (5)	$O_{4b}-O_{2d}$	2.46 (5)
$O_{1a}-P_1-O_{2a}$	115 (2)	$O_{1b}-P_2-O_{2b}$	107 (2)
$O_{1a}-P_1-O_{3a}$	108 (2)	$O_{1b}-P_2-O_{3b}$	111 (2)
$O_{1a}-P_1-O_{4a}$	104 (2)	$O_{1b}-P_2-O_{4b}$	108 (2)
$O_{2a}-P_1-O_{3a}$	106 (2)	$O_{2b}-P_2-O_{3b}$	104 (2)
$O_{2a}-P_1-O_{4a}$	114 (2)	$O_{2b}-P_2-O_{4b}$	110 (2)
$O_{3a}-P_1-O_{4a}$	111 (2)	$O_{3b}-P_2-O_{4b}$	115 (2)
$O_{1c}-P_3-O_{2c}$	113 (2)	$O_{1d}-P_4-O_{2d}$	105 (2)
$O_{1c}-P_3-O_{3c}$	116 (2)	$O_{1d}-P_4-O_{3d}$	114 (2)
$O_{1c}-P_3-O_{4c}$	105 (2)	$O_{1d}-P_4-O_{4d}$	105 (2)
$O_{2c}-P_3-O_{3c}$	111 (2)	$O_{2d}-P_4-O_{3d}$	108 (2)
$O_{2c}-P_3-O_{4c}$	104 (2)	$O_{2d}-P_4-O_{4d}$	108 (2)
$O_{3c}-P_3-O_{4c}$	109 (2)	$O_{3d}-P_4-O_{4d}$	116 (2)
$O_{1a}-H_{1a}-O^{i}_{1c}$	179 (27)	$O_{3a}-H_{1b}-O^{ii}_{3c}$	178 (39)
$O_{1b}-H_{1c}-O^{iii}_{1d}$	180 (20)	$O_{3b}-H_{1d}-O^{iv}_{3d}$	178 (34)
$O^{v}_{4b}-H_{2a}-O^{v}_{2d}$	178 (21)	$O_{2a}-H_{2b}-O^{vi}_{4c}$	178 (15)
$O^{v}_{2b}-H_{2c}-O^{vii}_{4d}$	179 (35)	$O^{vi}_{2c}-H_{2d}-O^{vi}_{4a}$	178 (12)
$O_{1a}-HO_{1a}-O^{i}_{1c}$	119	$O_{1c}-HO_{1c}-O^{i}_{1a}$	137
$O_{4c}-HO_{4c}-O^{viii}_{2a}$	119	$O_{2a}-HO_{2a}-O^{vi}_{4c}$	135
$O_{3a}-HO_{3a}-O^{ii}_{3c}$	118	$O_{3c}-HO_{3c}-O^{ii}_{3a}$	143
$O_{4a}-HO_{4a}-O_{2c}$	112	$O_{2c}-HO_{2c}-O_{4a}$	140
$O_{1b}-HO_{1b}-O^{iii}_{1d}$	122	$O_{1d}-HO_{1d}-O^{iii}_{1b}$	144
$O_{2b}-HO_{2b}-O^{vi}_{4d}$	108	$O_{4d}-HO_{4d}-O^{viii}_{2b}$	151
$O_{3b}-HO_{3b}-O^{iv}_{3d}$	127	$O_{3d}-HO_{3d}-O^{iv}_{3b}$	139
$O_{4b}-HO_{4b}-O_{2d}$	118	$O_{2d}-HO_{2d}-O_{4b}$	125

Symmetry codes: (i) $1-x, 1-y, -z$; (ii) $1-x, 1-y, 1-z$; (iii) $1-x, -y, -z$; (iv) $1-x, -y, -1-z$; (v) $x-1, y-1, z$; (vi) $x-1, y, z$; (vii) $x-2, y-1, z$; (viii) $1+x, y, z$.

the P—O distances). A further release of the distance restrictions showed no variation in the positions of H atoms. Such a hydrogen-bond scheme is shown in Fig. 7.

However, the P—O—H angles observed in this family of compounds contradict the accepted geometry of the dihydrogenphosphate ion, in which the P—O—H angle is nearly 109° and the O—H distance is 0.85 Å for X-rays. A force-field model of hydrogen bonding obtained with the program *HYDROGEN* (Nardelli, 1999) consistent with this geometry shows that all the O atoms involved in the hydrogen bonds can be considered as donor and acceptor. This would imply a disordered configuration of the PO_4 groups that has not been observed in other phases of TDP and DTDP. As expected, this model does not improve the above results because of the

presence of Tl atoms. The calculated coordinates of H atoms are given in the supplementary material. The bonding scheme is shown in Fig. 8.

The PO_4 tetrahedra are rather regular, as can be concluded from the P—O distances listed in Table 3. Decompositions of the displacements[6] of the P and O atoms in rigid rotations and translations of the PO_4 groups as a whole with respect to the common orthorhombic phase are shown in Table 4. The relatively high values of R_d indicate that the rigid-body approximation is rather rough, *i.e.* the internal distortion of the tetrahedra cannot be neglected. A comparison with a similar fit for the PO_4 groups at room temperature (Ríos, Paulus *et al.*, 1998) shows (taking R_d as indicator) that the tetrahedra deformation is larger than at room temperature but smaller than that observed in DTDP (see Table 4). Nevertheless the structural distortions of PO_4 groups in TDP and DTDP are quite different. On one hand, the translations of tetrahedra in TDP reproduce with small variations the ferroelastic distortion at room temperature (Ríos, 1997; Ríos, Paulus *et al.*, 1998). Rotations are also similar in structure to those at room temperature, R_x being the dominant one. R_y exhibits a noticeable increment, although it is still smaller (for three of the PO_4 tetrahedra) than the corresponding rotation in the antiferroelectric phase of DTDP. This seems to indicate indirectly that the ordering of the H1 atoms has not occurred (or not completed) yet.

Table 4
Rigid rotations (°) and translations (relative units) of the PO_4 groups with respect to the positions they occupy in the high-temperature phase (Ríos *et al.*, 1995) for TDP and DTDP.

The atomic displacements have been fitted as explained in the text. R_d is the agreement factor. Each tetrahedron is labeled by its central atom. In TDP, the four tetrahedra are symmetry independent. In DTDP, the pairs (P_1, P_2) and (P_3, P_4) are related by $\{C_{2z}|1/2,1/2,1/2\}$. The remaining four groups can be obtained by the application of an inversion center.

Group	R_x T_x	R_y T_y	R_z T_z	R_d (%)	R_x T_x	R_y T_y	R_z T_z	R_d (%)
P_1	−7.70	−5.41	−0.75	21	−4.81	3.59	0.02	22
	−0.024	0.005	−0.010		−0.017	−0.004	−0.005	
P_2	−9.09	1.46	−0.85	16	4.81	−3.59	0.02	22
	−0.037	0.001	0.022		0.017	0.004	−0.005	
P_3	−9.48	1.56	0.64	18	−2.58	−4.80	−0.29	27
	−0.024	−0.002	−0.018		−0.013	0.004	0.003	
P_4	−9.66	−0.44	0.73	25	2.58	4.80	−0.29	27
	−0.030	0.000	0.019		0.013	−0.004	0.003	

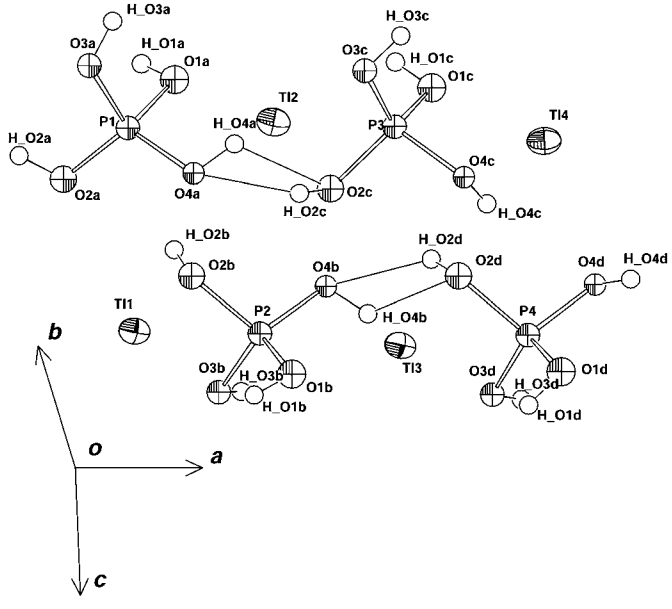

Figure 8
Bonding scheme derived from the calculated coordinates given in the supplementary material.

5. Conclusions

A structural model for the low-temperature phase of TDP has been refined. In spite of the difficulties derived from the presence of twin domains and the high (pseudo)symmetry of heavier atoms, the space group seems to be $P\bar{1}$. The inversion center is consistent with the lack of second-harmonic generation in this phase. The position of O and (in particular) H atoms could not be accurately determined because their contribution to the scattered intensity is almost negligible. Two different models for H atoms have been proposed. One of them has been based directly on the antiferroelectric phase of DTDP. The other comes from force-field calculations and it would imply an additional disorder of the PO_4 tetrahedra that has not been observed in DTDP or KDP. However, the presence of Tl does not permit us to distinguish between them. Therefore, no direct conclusion about the ordering of the H-type atoms can be stated.

Although the unit cell of TDP can be chosen to be metrically equivalent to that of DTDP at room temperature, their respective distortions with respect to the common high-temperature phase are different. In particular, the small rigid rotation around b of PO_4 groups indicates indirectly that the ordering of H1 atoms, which is thought to be completely correlated with the appearance of antiferroelectricity, is at least incomplete.

The expected isomorphism between this phase of TDP and the antiferroelectric phase of DTDP does not seem to occur. As noted by Pasquier *et al.* (1997), it could be recovered in a lower-temperature phase.

Professor M. Nardelli is particularly acknowledged for helpful discussions and the force-field calculations. EA is indebted to the Basque government for financial support. This work has been supported by the Basque government through the project PI97/71.

[6] The decomposition was realized by least squares. The minimized function was $\Sigma(d_o - d_c)^2$, where d_o and d_c are the observed and calculated atomic displacements, respectively. The agreement factor of the fit is defined as $R_d = [\Sigma(d_o - d_c)^2/\Sigma d_o^2]^{1/2}$.

References

Aizu, K. (1970). *J. Phys. Soc. Jpn*, **28**, 691–698.
Becker, M. (1995). Diplomarbeit im Fach Mineralogie, Institut für Kristallographie RWTH, Aachen, Germany.
Blinc, R. & Zeks, B. (1987). *Ferroelectrics*, **72**, 193–227.
Brese, N. E. & O'Keefe, M. (1991). *Acta Cryst.* B**47**, 192–197.
Brown, I. D. & Altermatt, D. (1985). *Acta Cryst.* B**41**, 244–247.
Cosier, J. & Glazer, A. M. (1986). *J. Appl. Cryst.* **19**, 105–107.
Davenport, G., Hall, S. & Dreissig, W. (2000). *ORTEP. Xtal*3.7 *System*, edited by S. R. Hall, D. J. du Boulay & R. Olthof-Hazekamp. University of Western Australia, Australia.
Kim, K.-B., Lee, K.-S. & Lee, C. (1998). *J. Phys. Soc. Jpn*, **67**, 1886–1889.
Lawrence, M. C. & Robertson, G. N. (1980). *J. Phys. C*, **13**, L1053–L1059.
McMahon, M. I., Nelmes, R. J., Kuhs, W. F., Dorwarth, R., Piltz, R. O. & Tun, Z. (1990). *Nature* (*London*), **348**, 317–319.
Matsubara, T. & Matsushita, E. (1984). *Prog. Theor. Phys.* **71**, 209–211.
Matsuo, T. & Suga, H. (1977). *Solid State Commun.* **21**, 923–927.
Nardelli, M. (1999). *J. Appl. Cryst.* **32**, 563–571.
Nelmes, R. J. (1981). *Solid State Commun.* **39**, 741–743.
Nelmes, R. J. & Choudary, R. N. P. (1978). *Solid State Commun.* **26**, 823–826.
Nelmes, R. J. & Choudary, R. N. P. (1981). *Solid State Commun.* **38**, 321–324.
Nelmes, R. J., Meyer, G. M. & Tibballs, J. E. (1982). *J. Phys. C*, **15**, 59–75.
Oddon, Y., Tranquard, A. & Pèpe, G. (1979). *Acta Cryst.* B**35**, 542–546.
Pasquier, B., Le Calvé, N. & Ouafik, Z. (1997). *Chem. Phys.* **223**, 33–50.
Petrícek, V. & Dusek, M. (2000). *The Crystallographic Computing System JANA*2000. Institute of Physics, Praha, Czech Republic.
Ríos, S. (1997). PhD thesis, Université Paris VI, France.
Ríos, S., Paulus, W., Cousson, A., Quilichini, M., Heger, G., Le Calvé, N. & Pasquier, B. (1995). *J. Phys. I France*, **5**, 763–769.
Ríos, S., Paulus, W., Cousson, A., Quilichini, M., Heger, G., Le Calvé, N. & Pasquier, B. (1998). *Acta Cryst.* B**54**, 790–797.
Ríos, S., Paulus, W., Cousson, A., Quilichini, M., Pasquier, B., Le Calvé, N. & Heger, G. (1996). *Ferroelectrics*, **185**, 177–180.
Ríos, S., Quilichini, M., Knorr, K. & André, G. (1999). *Physica B*, **266**, 290–299.
Ríos, S., Quilichini, M. & Pérez-Mato, J. M. (1998). *J. Phys. Condens. Matter*, **10**, 3045–3060.
Rodriguez-Carvajal, J. (1999). *FullProf.* Version 0.5. Laboratoire Léon Brillouin, CEA-CNRS, Saclay, France.
Salje, E. K. H. (1990). *Phase Transitions in Ferroelastic and Coelastic Crystals*, pp. 25–26. Cambridge University Press.
Sapriel, J. (1975). *Phys. Rev. B*, **12**, 5128–5139.
Seliger, J., Zagar, V. & Blinc, R. (1987). *J. Chem. Phys.* **88**, 3260–3262.
Shuvalov, L. A. (1985). *Ferroelectrics*, **65**, 143–152.
Stoe & Cie (1998). *Stoe IPDS Software.* Version 2.87. Stoe and Cie GmbH, Darmstadt, Germany.
Sugimoto, N. & Ikeda, S. (1991). *Phys. Rev. Lett.* **67**, 1306–1309.
Yasuda, N., Fujimoto, S. & Asano, T. (1980). *Phys. Lett. A*, **76**, 174–176.
Yasuda, N., Fujimoto, S., Asano, T., Yoshino, K. & Inushi, Y. (1980). *J. Phys. D*, **13**, 85–94.
Yoshida, H., Endo, M., Kaneko, T., Osaka, T. & Makita, Y. (1984). *J. Phys. Soc. Jpn*, **53**, 910–912.